Journal of Power Sources 196 (2011) 1097–1102

Contents lists available at ScienceDirect

Journal of Power Sources

journal homepage: www.elsevier.com/locate/jpowsour

Mesh optimization for microbial fuel cell cathodes constructed around stainless steel mesh current collectors

Fang Zhang[a], Matthew D. Merrill[a], Justin C. Tokash[a], Tomonori Saito[a,b], Shaoan Cheng[a,c], Michael A. Hickner[b], Bruce E. Logan[a,*]

[a] Department of Civil and Environmental Engineering, Penn State University, 212 Sackett Building, University Park, PA 16802, USA
[b] Department of Materials Science and Engineering, Penn State University, Steidle Building, University Park, PA 16802, USA
[c] State Key Laboratory of Clean Energy Utilization, Department of Energy Engineering, Zhejiang University, Hangzhou 310027, PR China

ARTICLE INFO

Article history:
Received 14 July 2010
Received in revised form 9 August 2010
Accepted 10 August 2010
Available online 17 August 2010

Keywords:
Microbial fuel cell
Cathode
Current collector
Stainless steel mesh
Electrochemical impedance spectroscopy

ABSTRACT

Mesh current collectors made of stainless steel (SS) can be integrated into microbial fuel cell (MFC) cathodes constructed of a reactive carbon black and Pt catalyst mixture and a poly(dimethylsiloxane) (PDMS) diffusion layer. It is shown here that the mesh properties of these cathodes can significantly affect performance. Cathodes made from the coarsest mesh (30-mesh) achieved the highest maximum power of $1616 \pm 25\ mW\ m^{-2}$ (normalized to cathode projected surface area; $47.1 \pm 0.7\ W\ m^{-3}$ based on liquid volume), while the finest mesh (120-mesh) had the lowest power density ($599 \pm 57\ mW\ m^{-2}$). Electrochemical impedance spectroscopy showed that charge transfer and diffusion resistances decreased with increasing mesh opening size. In MFC tests, the cathode performance was primarily limited by reaction kinetics, and not mass transfer. Oxygen permeability increased with mesh opening size, accounting for the decreased diffusion resistance. At higher current densities, diffusion became a limiting factor, especially for fine mesh with low oxygen transfer coefficients. These results demonstrate the critical nature of the mesh size used for constructing MFC cathodes.

1. Introduction

Microbial fuel cells (MFCs) are devices that use bacteria as catalysts to oxidize organic or inorganic matter and generate current [1–5]. One promising application for MFCs is wastewater treatment, where energy is recovered from organic matter while at the same time the wastewater is treated. Many chemicals have been used as electron acceptors in MFCs, but oxygen is the most cost-effective, sustainable and environmental friendly electron acceptor for wastewater treatment applications. Air cathodes, which have one side exposed to air and the other exposed to wastewater, provide an efficient method for transferring oxygen to the cathode catalytic sites. Oxygen used at the cathode is readily replenished directly from air without the need for wastewater aeration [6].

The power densities produced by MFCs are mainly limited by the cathode performance and high ohmic resistance of these systems [7,8]. Cathode design is challenging due to the relatively poor kinetics of oxygen reduction reaction under neutral pH conditions in MFCs, compared to hydrogen fuel cells where cathodes work at much lower pH [9]. Improving cathode performance is therefore critical for increasing power production in MFCs by changes in system architecture that reduce internal resistance, such as by reducing electrode spacing and increasing solution conductivity [10,11]. However, the most critical factor in the development of new cathodes for MFCs is to use inexpensive materials that lack precious metals.

Metal current collectors are usually needed for fuel cell electrodes especially for large-scale systems to avoid large in-plane resistances across the electrode area, and therefore MFC electrodes are being constructed around inexpensive current collectors. For example, graphite fiber brush electrodes have a twisted metal core to facilitate electron transfer from the bacteria to the circuit. Using this type of anode a maximum power density of $2400\ mW\ m^{-2}$ was produced in a small laboratory-scale reactor [12]. Stainless steel (SS) mesh has been used as a cathode current collector [13,14]. By adding a SS mesh to the surface of an anion exchange membrane coated with a conductive graphite paint, power was increased from $450\ mW\ m^{-2}$ to $575\ mW\ m^{-2}$ [14]. It was recently shown that the current collector could be directly integrated into the cathode structure by constructing the cathode around the current collector. Inexpensive activated carbon (AC) and a polytetrafluoroethylene (PTFE) binder were pressed onto a Ni mesh, with an additional PTFE layer serving as a diffusion layer. This AC cathode produced a maximum of $1220\ mW\ m^{-2}$, despite the lack of a metal catalyst [15]. A different type of mesh cathode was constructed using SS mesh by coating one side of the mesh with a poly(dimethylsiloxane) (PDMS)

* Corresponding author. Tel.: +1 814 863 7908; fax: +1 814 863 7304.
E-mail address: blogan@psu.edu (B.E. Logan).

0378-7753/$ – see front matter © 2010 Elsevier B.V. All rights reserved.
doi:10.1016/j.jpowsour.2010.08.011

Table 1
R_{ct}, R_d and capacitance at OCP, 0.1 V and 0 V with cathode made from mesh of different sizes.

Mesh size (N in.$^{-1}$)	30	50	70	90	120
Opening size (mm)	0.53	0.28	0.20	0.15	0.12
Wire diameter (mm)	0.30	0.23	0.17	0.14	0.09
Fractional open area (%)	40.8	30.3	29.8	25.4	30.5
Porosity	0.70	0.61	0.61	0.57	0.62
Specific surface area (mm^{-1})	3.9	6.8	9.5	12.4	16.2
R_{ct} ($\Omega\,cm^2$)					
OCP	4.9	3.7	5.1	5.4	6.6
0.1 V	1.6	1.7	3.1	3.6	5.1
0 V	0.04	0.03	0.02	0.74	1.3
R_d ($\Omega\,cm^2$)					
OCP	6.6	8.7	12.4	10.8	12.2
0.1 V	0.6	1.0	0.6	1.2	1.4
0 V	1.0	1.1	0.8	12.2	12.6
C ($\Omega^{-1}\,s^n\,cm^{-2}$)					
OCP	1.42	1.06	0.95	0.81	0.50
0.1 V	2.12	1.20	1.30	0.98	0.74
0 V	1.05	0.81	0.87	0.97	0.65
n					
OCP	0.79	0.82	0.89	0.90	0.86
0.1 V	0.70	0.72	0.73	0.75	0.71
0 V	0.36	0.42	0.49	0.81	0.81

and carbon black diffusion layer (air side) and the other side with a Pt/C catalyst layer [13]. Power densities were optimized by limiting oxygen diffusion by varying the number of PDMS/carbon black diffusion layers. The optimum condition was two diffusion layers, which produced power densities of 1610 mW m^{-2} [13]. In both of these studies the effect of the mesh size on the electrode was not considered. However, the opening size and amount of metal used in the mesh could affect oxygen transfer, proton transfer, electrical conductivity, and relative contact between the coatings and metal surfaces, all of which can affect cathode performance.

In this study, we examined the effect of mesh size on cathode performance for SS mesh having five different sizes, with all mesh containing the same PDMS/carbon black diffusion layers and Pt/C catalyst. The different mesh cathodes were analyzed for power production, resistances due to cathode charge transfer and diffusion, electrode capacitance, and oxygen transfer.

2. Materials and methods

2.1. Cathodes

Cathodes were constructed from stainless steel mesh, Pt, and PDMS as previously described [13]. SS woven wire (plain weave) sizes, characterized by the number of openings per linear inch (from coarse to fine) were: 30 × 30, 50 × 50, 70 × 70, 90 × 90 and 120 × 120 (Table 1, type 304 SS, McMaster-Carr, OH). Mesh characteristics of openings per linear inch, wire diameter, opening size and fractional open area were specified by the manufacturers. Specific surface area (surface area per unit volume ratio) and porosity of the mesh (void fraction) were calculated based on the assumption that the mesh thickness was twice that of the individual wire diameters, and that the wires were uniformly cylindrical and in point-to-point contact. Two layers of PDMS/carbon black were applied to the air side as diffusion layers [13]. After applying the diffusion layer, the Pt catalyst layer with a nominal loading of 0.5 mg per cm^2 of cathode projected area (5 mg cm^{-2} 10% Pt on Vulcan XC-72 with 33.3 μL cm^{-2} of 5 wt% Nafion solution as binder) was applied to the SS mesh on the side facing the solution [8].

2.2. MFC construction and operation

MFCs were single-chamber cubic-shaped reactors constructed as previously described [16], with an anode chamber 4 cm long and 3 cm in diameter. The anode was a single ammonia gas treated graphite fiber brush (25 mm diameter × 25 mm length; fiber type PANEX 33 160K, ZOLTEK) [12,17]. All reactors were inoculated using the effluent from an MFC operated for over two years. The medium contained sodium acetate as the fuel (1.0 g L^{-1}), and a phosphate buffer nutrient solution (PBS; conductivity of 6.82 mS cm^{-1}) containing: Na_2HPO_4, 4.58 g L^{-1}; $NaH_2PHO_4{\cdot}H_2O$ 2.45 g L^{-1}; NH_4Cl 0.31 g L^{-1}; KCl 0.13 g L^{-1}; trace minerals (12.5 mL L^{-1}) and vitamins (5 mL L^{-1}) [18]. Reactors were all operated in fed-batch mode at 30 °C and were refilled each time when the voltage decreased to less than 20 mV forming one complete cycle of operation.

2.3. Calculations and measurements

Voltage (E) across the external resistor (1 kΩ, except as noted) in the MFC circuit was measured at 20 min intervals using a data acquisition system (2700, Keithley Instrument, OH) connected to a personal computer. Current ($I = E/R$) and power ($P = IE$) were calculated as previously described [3], with the current density and power density normalized by the projected surface area of the cathode. To obtain the polarization and power density curves as a function of current, external circuit resistances were varied from 1000 to 20 Ω in decreasing order every 20 min.

Physical characteristics of woven wire mesh can affect reactor performance, as shown in other engineered systems such as catalytic reactors and filters [19–21]. The wire diameter and the fractional opening (porosity) of a typical screen are the most significant factors. Under static flow conditions (no advective transport though the mesh), transport by diffusion can be modeled using $D_{Cj,p} = D_{Cj}\,(\theta/\tau_f)$ (macroporous matrix diffusion model), where $D_{Cj,p}$ is the diffusion constant for chemical C in the porous matrix filled with phase j, D_{Cj} the diffusion constant for chemical C in phase j, θ the porosity of the porous medium, and τ_f the tortuosity factor [22]. For plain weaves the fluid path length and the screen thickness are essentially equal and $\tau_f = 1$ [19]. In order to assess how mesh porosity affected mesh mass transfer properties, oxygen permeability was measured in terms of oxygen transfer coefficient as previously described using the same 4-cm reactor examined in MFC tests [23]. Dissolved oxygen concentrations were measured using a non-consumptive oxygen probe (NeoFox, Ocean Optics, Inc., Dunedin, FL).

The mesh characteristics can also be expected to affect charge transfer and current distribution in cathodes. Electrochemical impedance spectroscopy (EIS) can be used to characterize electrode properties and measure the MFC internal resistance R_{int} [24–26]. Electrochemical properties including three sources of resistance: charge transfer resistance (R_{ct}), diffusion resistance (R_d), solution resistance (R_s), and capacitance of the catalyst double layer are determined by fitting the measured impedance data to an equivalent circuit.

Linear sweep voltammetry (LSV) and EIS were used to electrochemically characterize the cathodes using a potentiostat (PC4/750, Gamry Instruments). Cathodes were placed in an electrochemical cell consisting of a working electrode (cathode with 7 cm^2 projected surface area), an Ag/AgCl reference electrode (RE-5B; BASi, West Lafayette, IN) and a Pt counter electrode [13]. For LSV tests, the cathode was equilibrated to +0.5 V for 1 h and then scanned at −1 mV s^{-1} to 0 V (vs. standard hydrogen electrode, SHE) with current interrupt IR compensation to dynamically correct uncompensated resistance errors. Impedance measurements were conducted at open circuit and polarized conditions which were 0.1 V and 0 V versus SHE

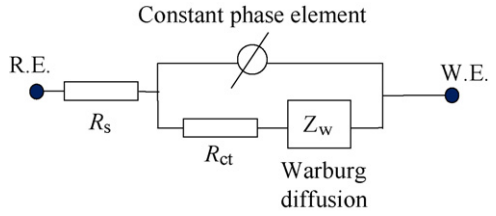

Fig. 1. Equivalent circuit of the electrochemical cell for EIS.

(−0.1 V and −0.2 V vs. Ag/AgCl) over a frequency range of 100 kHz to 1 mHz with a sinusoidal perturbation of 10 mV amplitude. Resistances and capacitances were normalized to cathode projected surface area.

EIS spectra were fitted into an equivalent circuit using Gamry Echem Analyst software (provided by the potentiostat manufacturer). The equivalent circuit used here assumes that the cathode reaction is affected by both reaction kinetics and diffusion (Fig. 1), with the symbol R_s for solution resistance and R_{ct} for charge transfer resistance. A constant phase element (CPE) was used instead of a capacitor in order to model double layer capacitance when surface roughness or a distribution of reactions across the surface can affect overall kinetics. The CPE has two parameters: C and n. C indicates the capacitance, and it is the value of the admittance at $\omega = 1$ rad s^{-1} (~0.16 Hz). The phase angle depression factor, n, has a value between 0 and 1 and it describes the level of ideality for the CPE circuit element ($n = 1$ is perfectly ideal capacitive behavior). A porous bounded Warburg element was used to evaluate diffusion resistance in terms of two parameters: Y_0 and B. Y_0 is the magnitude of the admittance at $\omega = 1$ rad s^{-1}, while B characterizes the time it takes for a reactant to diffuse through a thin film, which in our case is the thin film of electrolyte between the electrode and the permeable PDMS membrane. The ratio B/Y_0 indicates the magnitude of diffusion resistance R_d.

3. Results

3.1. Performance of SS mesh cathodes in MFCs with different mesh sizes

Large differences in power production by cathodes with different mesh size were observed based on polarization data. MFCs with 30-mesh cathodes achieved the highest power density of 1616 ± 25 mW m^{-2} (±S.D., duplicate reactors), which was similar to that produced with 50-mesh of 1563 ± 128 mW m^{-2} (Fig. 2A). Cathodes made from 70-mesh achieved a slightly lower power density of 1415 ± 125 mW m^{-2}. Power production was much lower when smaller mesh opening sizes were used, with 982 ± 62 mW m^{-2} for the 90-mesh and 599 ± 57 mW m^{-2} for the 120-mesh (Fig. 2A). Cathode potentials followed the same trend as the power production, and anode potentials were all similar, providing evidence that the cathode performance was the reason for the differences in power generation among these reactors (Fig. 2B).

3.2. LSV tests

SS mesh cathodes with different mesh size were examined using LSV to evaluate the effect of SS mesh size on electrochemical performance in the absence of bacteria. Current densities of cathodes increased in magnitude with increasing mesh opening sizes and with increasing overpotentials (Fig. 3). Cathodes made from 30- and 50-mesh had similar current densities across the higher scanned potentials, while 50-mesh performed slightly better at low potentials. Current densities of the SS mesh cathodes with smaller mesh openings had reduced activities compared to the coarser meshes,

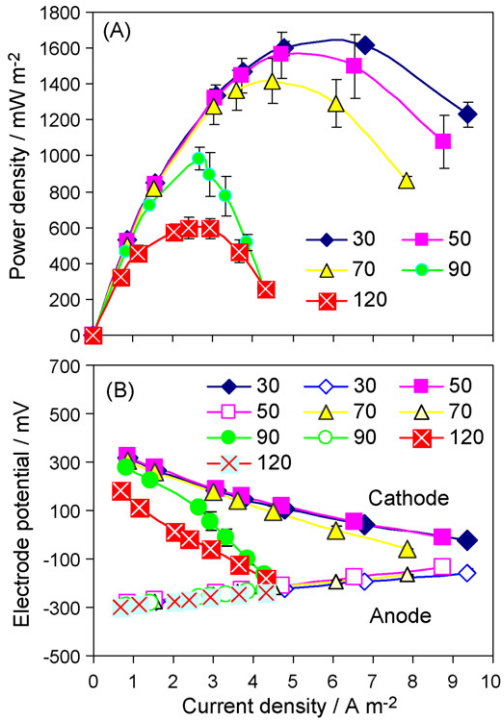

Fig. 2. (A) Power densities and (B) electrode potentials of SS mesh cathodes with different mesh size as a function of current density (normalized to cathode projected surface area) obtained by varying the external circuit resistance (1000–20 Ω). (Error bars ± SD based on measurement of two duplicate reactors.).

and the cathode made from the finest mesh (120-mesh) had the lowest current response at any given scanned potential (Fig. 3). These scans demonstrate inherent differences in electrochemical properties of cathodes based on their mesh (opening) sizes.

3.3. Impedance of the cathodes

EIS was performed at open circuit and polarized conditions of 0.1 V and 0 V. Open circuit cathode potential ranged between 0.354 V and 0.385 V (vs. SHE) from fine to coarse mesh. Internal resistance decreased with an increase in mesh opening size (from fine to coarse mesh, Figs. 4 and 5), which is due to differences in current density at the various fixed potentials under consideration. This behavior is shown by a decrease in the size of the semi-circle produced in Nyquist plots (Fig. 4). As expected, solution resistances (R_s) were all similar for the cathodes at different polarized conditions due to the use of the same cell configuration and solution in EIS tests (Fig. 5). However, other electrochemical properties (R_{ct}, R_d

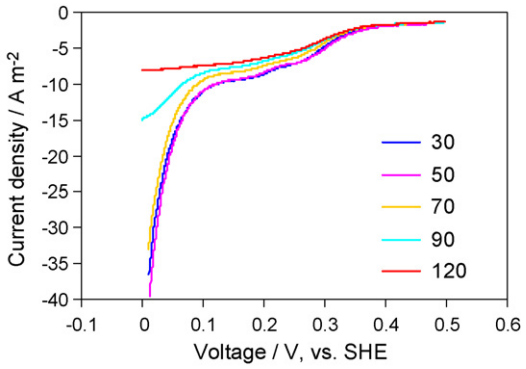

Fig. 3. LSV of SS mesh cathodes with different mesh size.

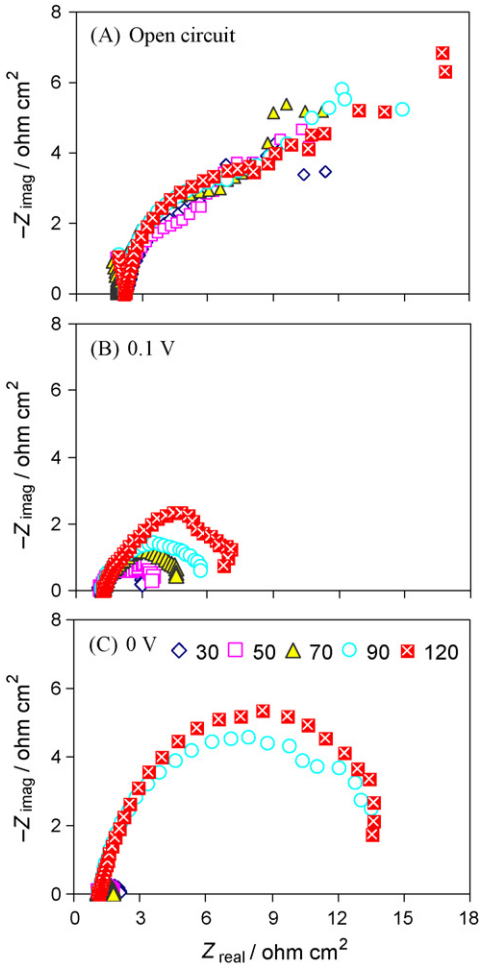

Fig. 4. Nyquist plots of EIS spectra by SS mesh cathodes with different mesh size at (A) open circuit, (B) 0.1 V, and (C) 0 V. (Resistances normalized to cathode projected surface area.)

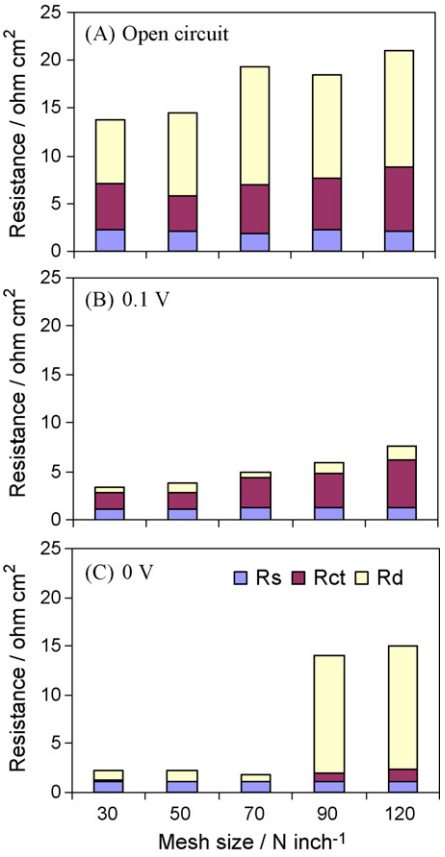

Fig. 5. Component analysis of internal resistance at different EIS operation conditions for cathodes with different sized mesh: (A) open circuit, (B) 0.1 V, and (C) 0 V. (Resistances normalized to cathode projected surface area.)

and double layer capacitance) were altered by the use of cathodes with different sized mesh. R_{ct} generally decreased with increasing mesh opening size, and decreased with increasing oxygen reduction overpotential (OCP → 0.1 V → 0 V; Fig. 5). At 0.1 V, the cathode made from 30-mesh had the smallest R_{ct} of 1.6 Ω cm^2 while 120-mesh had the largest of R_{ct} = 5.1 Ω cm^2. These values decreased to R_{ct} = 0.04 Ω cm^2 (30 mesh) and 1.3 Ω cm^2 (120 mesh) at the higher overpotential (0 V).

Diffusion resistances also decreased from fine to coarse mesh at open circuit and polarized conditions. R_d decreased from 1.4 Ω cm^2 to 0.6 Ω cm^2 as mesh size decreased from 120- to 30-mesh (0.1 V). At the higher overpotential (0 V), R_d had larger variations with mesh size, with R_d = 12.2 Ω cm^2 for 90-mesh, and R_d = 12.6 Ω cm^2 for 120-mesh. These values are an order of magnitude larger than those of other coarser mesh cathodes (all <1.2 Ω cm^2) (Table 1, Fig. 5C). Thus, the increase in the diameter of the semi-circle in Nyquist plots when EIS was performed at 0 V compared to 0.1 V, was mainly due to the increase of R_d (Fig. 4B and C).

Double layer capacitance increased from fine to coarse mesh at both open circuit and polarized conditions (Table 1). This increase was due to more charge buildup at the interface between electrode and electrolyte because of higher current densities achieved by coarser mesh cathodes. It was also likely that coarser mesh cathodes produced more interface between electrode and electrolyte.

3.4. Oxygen permeability

Cathodes with different mesh size had different oxygen permeabilities, likely due to hindered diffusion by the mesh. Oxygen transfer coefficients increased with increasing opening size of mesh. Cathodes made from 30-mesh had the highest oxygen transfer coefficient of $2.2 \pm 0.2 \times 10^{-3}$ cm s^{-1} and finer mesh had lower values from $2.1 \pm 0.2 \times 10^{-3}$ cm s^{-1} (50-mesh) to $1.7 \pm 0.1 \times 10^{-3}$ cm s^{-1} (120-mesh) (Fig. 6). It was expected from the macroporous matrix diffusion model that the oxygen transfer coefficient would have a linear relationship against mesh porosity, and this was shown by general good agreement between predicted (based on the initial experimental value for the 30-mesh sample) and experimental oxygen transfer coefficients. However,

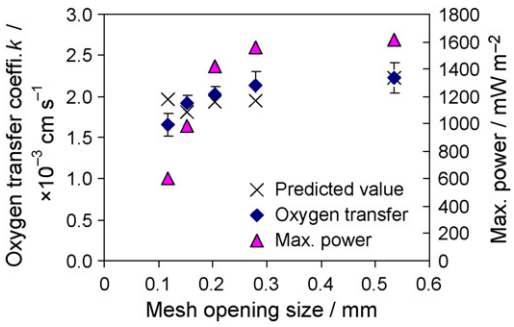

Fig. 6. Experimental and predicted oxygen transfer coefficient (based on the macroporous matrix diffusion model) of SS mesh cathodes with different sized mesh, and maximum power densities achieved by these cathodes, against mesh opening size.

maximum power production increased much more rapidly than the oxygen transfer coefficients with the increasing mesh opening size from 0.1 mm to 0.3 mm (Fig. 6), suggesting that other characteristics of the system such as wire diameter and contact between metal and catalyst, affected overall power production. Additional comparisons of oxygen transfer to porosity and fractional open area did not explain the observed increases in power (see Supporting Information).

4. Discussion

Reactor performance generally increased with increasing mesh opening size from fine to coarse mesh. The best performance was obtained with SS mesh cathodes made using 30-mesh, resulting in a maximum power density of $1616 \pm 25\ mW\ m^{-2}$ ($47.1 \pm 0.7\ W\ m^{-3}$). Cathodes made from 50-mesh had similar performance to those made with 30-mesh, but the use of finer mesh resulted in less power production and lower cathode potentials. Cathode made from 90-mesh produced $982 \pm 62\ mW\ m^{-2}$, which was lower than that obtained in previous tests ($1610 \pm 56\ mW\ m^{-2}$) [13], primarily due to differences in solution conductivity ($8.2\ mS\ cm^{-1}$ compared to $6.8\ mS\ cm^{-1}$ here), but also perhaps the use of different inocula and variations in materials (different batches of stainless steel mesh).

Both electrochemical studies and MFC tests show that mesh properties can appreciably affect MFC performance. Coarser mesh cathodes exhibited higher current densities in LSV voltammograms and produced higher power in MFCs, due to lower values of both R_{ct} and R_d. R_s were all similar among all the cathodes, and this solution resistance can be reduced by minimizing the space between anode and cathode using a separator [27,28]. When EIS was conducted at a fixed cathode potential of 0.1 V, close to the point of maximum power production for most cathodes in MFC tests (Fig. 2B), R_{ct} was the largest contributor to resistance, indicating that the cathode reaction was primarily kinetically limited under our operating conditions. Kinetic limitations suggest that improving oxygen reduction kinetics is important for improving MFC performance. Comparing R_{ct} at different potentials, a higher oxygen reduction overpotential resulted in a lower R_{ct} because of the larger driving force for electron transfer. At a given potential, coarser mesh cathodes had lower R_{ct} values than the finer mesh. There are two possible reasons for this difference. One is that coarser mesh with larger wire diameter had more mesh/catalyst contacts which would lower the resistance for electrons going across metal surface and distributing among catalyst sites. The other possible reason is that catalysts could be more effective in oxygen reduction on coarser mesh cathodes, as inferred from the variation in double layer capacitance of the cathodes as discussed below.

Double layer capacitance can be related to the electrode–electrolyte networks in the catalytic layer because capacitance is induced by the buildup of charge at the electrode–electrolyte interface. Measurement of the double layer capacitance can be used as an *in situ* assessment of the wetted surface area, i.e. the electroactive surface area [29,30]. In this study, double layer capacitance increased from 120-mesh to 30-mesh, suggesting that the coarser mesh had larger active surface area and thus a higher catalyst utilization. It is possible that a coarse mesh allows more catalyst/mesh contacts as the catalyst layer "sinks" into the openings of the mesh, while the catalyst layer sits on top of the fine mesh. In that case, the catalyst layer on coarse mesh coats more of the wires and produces more catalyst/mesh contacts, so that the coarse mesh can produce more interface between the metal surface, catalyst layer, and the electrolyte. Larger currents achieved by coarser mesh also contributed to more surface charge buildup, resulting in a higher capacitance for the coarser mesh cathodes.

Oxygen transfer through cathodes was hindered by the impermeable SS mesh, with measured mass transfer coefficients in general agreement with diffusion calculations. The lack of agreement with the model for this oxygen transfer coefficient was possibly a result of the impact of overall diffusion rates in the microporous PDMS and carbon black layer rather than mass transfer controlled by overall porosity of the SS mesh openings. The variations in cathode oxygen permeabilities resulted in different R_d values, with coarser mesh having higher oxygen transfer coefficients and lower R_d values. When EIS was conducted at 0 V, the R_d was much larger than R_{ct} (Fig. 5C), and diffusion limitations became the dominant factor affecting cathode performance. We observed that the R_d values for the 90-mesh and 120-mesh cathodes substantially increased at 0 V, most likely due to oxygen depletion at the high current densities. Therefore, 30-, 50-, 70-mesh cathodes with much less R_d exhibited much higher current densities at 0 V in LSV tests (due to a lack of oxygen diffusion limitations in these mesh cathodes) compared to finer mesh cathodes (90- and 120-mesh).

5. Conclusions

These experiments have shown that SS mesh can appreciably affect the cathode performance. By selecting commercially available SS mesh with different mesh size numbers, mesh properties such as opening size, wire diameter, surface area all varied. These changes in properties affected oxygen transfer and the efficiency of catalyst, as indicated by a change in the double layer capacitance, charge transfer resistance, and diffusion resistance of the cathodes. MFC performance was primarily kinetics limited for our operating conditions, and this was the main reason for the variations in MFC performance with the different SS mesh cathodes. Oxygen transfer hindrance through the mesh was more related to opening size of the SS mesh, and this hindrance further affected the diffusion resistance of the cathodes. Cathode oxygen reduction rates were limited by diffusion at higher current densities, however, especially for the fine mesh. Coarse mesh provided the best performance, and the maximum power production reached a plateau when we increased the mesh opening size (Fig. 6). Therefore, based on our experiments the 30- or 50-mesh are the most optimal materials for maximizing power production. These coarse meshes also have better mechanical strength because of the larger diameter wires used for fabrication, favoring their use in practical applications as current collectors in MFC cathodes.

Acknowledgments

The authors thank David Jones and Ellen Bingham for help with the analytical measurements. This research was supported by Award KUS-I1-003-13 from the King Abdullah University of Science and Technology (KAUST).

Appendix A. Supplementary data

Supplementary data associated with this article can be found, in the online version, at doi:10.1016/j.jpowsour.2010.08.011.

References

[1] B.E. Logan, Microbial Fuel Cells, John Wiley & Sons Inc., Hoboken, NJ, 2008.
[2] B.E. Logan, Nat. Microbiol Rev. 7 (2009) 375–381.
[3] B.E. Logan, P. Aelterman, B. Hamelers, R. Rozendal, U. Schröder, J. Keller, S. Freguiac, W. Verstraete, K. Rabaey, Environ. Sci. Technol. 40 (2006) 5181–5192.
[4] D.R. Lovley, Nat. Microbiol. Rev. 4 (2006) 497–508.
[5] K. Rabaey, W. Verstraete, Trends Biotechnol. 23 (2005) 291–298.
[6] H. Liu, R. Ramnarayanan, B.E. Logan, Environ. Sci. Technol. 38 (2004) 2281–2285.
[7] B. Kim, I. Chang, G. Gadd, Appl. Microbiol. Biotechnol. 76 (2007) 485–494.
[8] S. Cheng, H. Liu, B.E. Logan, Environ. Sci. Technol. 40 (2006) 364–369.

[9] G.C. Gil, I.S. Chang, B.H. Kim, M. Kim, J.K. Jang, H.S. Park, H.J. Kim, Biosens. Bioelectron. 18 (2003) 327–334.
[10] H. Liu, S. Cheng, B.E. Logan, Environ. Sci. Technol. 39 (2005) 5488–5493.
[11] S. Cheng, H. Liu, B.E. Logan, Environ. Sci. Technol. 40 (2006) 2426–2432.
[12] B.E. Logan, S. Cheng, V. Watson, G. Estadt, Environ. Sci. Technol. 41 (2007) 3341–3346.
[13] F. Zhang, T. Saito, S. Cheng, M.A. Hickner, B.E. Logan, Environ. Sci. Technol. 44 (2010) 1490–1495.
[14] Y. Zuo, S. Cheng, B.E. Logan, Environ. Sci. Technol. 42 (2008) 6967–6972.
[15] F. Zhang, S. Cheng, D. Pant, G.V. Bogaert, B.E. Logan, Electrochem. Commun. 11 (2009) 2177–2179.
[16] H. Liu, B.E. Logan, Environ. Sci. Technol. 38 (2004) 4040–4046.
[17] S. Cheng, B.E. Logan, Electrochem. Commun. 9 (2007) 492–496.
[18] S. Cheng, D. Xing, D.F. Call, B.E. Logan, Environ. Sci. Technol. 43 (2009) 3953–3958.
[19] J.C. Armour, J.N. Cannon, AlChE J. 14 (1968) 415–420.
[20] C.N. Satterfield, D.H. Cortez, Ind. Eng. Fundam. Chem. 9 (1970) 613–620.
[21] A. Kolodziej, J. Lojewska, Chem. Eng. Process. 48 (2009) 816–822.
[22] B.E. Logan, Environmental Transport Processes, Wiley, New York, 1999.
[23] S. Cheng, H. Liu, B.E. Logan, Electrochem. Commun. 8 (2006) 489–494.
[24] Z. He, F. Mansfeld, Energy Environ. Sci. 2 (2009) 215–219.
[25] A.K. Manohar, O. Bretschger, K.H. Nealson, F. Mansfeld, Bioelectrochemistry 72 (2008) 149–154.
[26] A.K. Manohar, F. Mansfeld, Electrochim. Acta 54 (2009) 1664–1670.
[27] Y. Fan, H. Hu, H. Liu, J. Power Sources 171 (2007) 348–354.
[28] X. Zhang, S. Cheng, X. Wang, X. Huang, B.E. Logan, Environ. Sci. Technol. 43 (2009) 8456–8461.
[29] A.D. Eaton, L.S. Clesceri, A.E. Greenberg, Standard Methods for the Examination of Water and Wastewater. 19 ed. APHA, AWWA, WEF, Washington, DC, 1995.
[30] S. Jarek, J. Thonstad, J. Appl. Electrochem. 17 (1987) 1203–1212.